Conception of an underwater prototype array: from simulation design to mechanical assessment

Joffrey Jaumont, Valentin Baron, Barbara Nicolas, Florent Fayet, Arthur Finez, Jerome I. Mars

Conception of an underwater prototype array: from simulation design to mechanical assessment.

Joffrey Jaumont
OSEAN SAS
ZAE La Bayette
83220, Le Pradet, France
joffrey.jaumont@osean.fr

Valentin Baron
MicrodB
28, Chemin du Petit Bois
69134 Ecully Cedex, France
valentin.baron@microdb.fr

Barbara Nicolas
Univ Lyon, INSA-Lyon,
Université Claude Bernard Lyon
1, UJM-Saint Etienne, CNRS,
Inserm, CREATIS, UMR 5220,
U1206, F-69100, LYON, France
barbara.nicolas@creatis.insa-lyon.fr

Florent Fayet
OSEAN SAS
ZAE La Bayette
83220 Le Pradet, France
florent.fayet@osean.fr

Arthur Finez
MicrodB
28, Chemin du Petit Bois
69134 Ecully Cedex, France
arthur.finez@microdb.fr

Jérôme Mars
Univ. Grenoble Alpes, CNRS,
Grenoble-INP, GIPSA-Lab
38000, Grenoble, France
jerome.mars@gipsa-lab.grenoble-inp.fr

***Abstract*—As natural resources are increasingly difficult to find on the surface of the earth, mining industries start to dig in deep waters to find new deposits. The production of noise in the surrounding environment is a direct consequence of this activity and it must be monitored to predict its impact on the nearby marine life. This is the goal of Abysound research project in which a monitoring system is conceived and used to localize and quantify deep underwater acoustic sources and propagate the sound they emit to create noise impact maps. This study focuses on the conception of the acoustic array which enables the localization of the sources. Given the harsh conditions of utilization, it must be ensured that from the design phase to the real deployment all the array parts are mechanically stable and they allow to perform acoustic computations accurately. After a presentation of the array shape and the mechanical constraints given as an input of the construction, the stability of the chosen structure is assessed. Firstly numerical simulations are performed to validate the stability. Then a deployment test is conducted in shallow waters and it shows both the mechanical stability of the array during a real launching and the effectiveness of the array to perform acoustic source localization thanks to an immersed source producing noise during the experiment.**

Keywords — acoustic array, deep sea mining, mechanical assessment.

I. Introduction

Due to the increasing demand of natural deposits for various industry purposes, underwater mining sites are becoming feasible and companies start to develop digging procedures at places around the globe where these minerals are present [1]. However as one can easily understand, these activities produce lots of noise that can disturb the rich marine life these sites shelter [2]. In order to control the emitted noise and predict its expected impact, the research project Abysound aims at creating a monitoring system composed of an acoustic array located in deep waters near the noisy zones to record the localization and the level of present acoustic sources. Then by computing the propagation of the identified sources, acoustic impact maps are determined to prevent the disturbance of the marine life.

This paper focuses on the conception of such an array. For a real industrial application it means producing an array that is able to localize and quantify acoustic sources that emit on a large bandwidth [100 Hz; 2 kHz] on the seafloor. These conditions are scaled according to the research project means at disposal leading in this study to a smaller array that searches for sources emitting on the frequency band [350 Hz, 7 kHz]. Acoustic array conception can be divided in two main steps starting with the hydrophone geometry arrangement to achieve aimed acoustic performances. It is followed by the array construction that must be accurate and robust enough to guarantee the expected performances while not interfering with the surrounding acoustic field.

Two principal options allow to realize an array design. Although different in their concept, they both need to evaluate a design from another using given metrics. On one hand hydrophone arrangements optimization using metaheuristic methods allows to converge up to the best configuration by minimizing a given functional combining these metrics [3][4]. This option is suited to find out unpredictable configurations in large search spaces but reaching only sub-optimal ones. On the other hand the solution space can be sampled as densely as possible according to the allowed configurations and all the yielded ones can be ranked using the given metrics in a more visible way [5]. This second option is more adapted to small

search spaces in which almost all configurations can be investigated in order to point out the best.

Once the design is produced, the array itself must be built. A perfect array would be just hydrophones set at the indicated location of the previous design. Nevertheless a structure is mandatory to put all the elements in place along with all the required electronics. The purpose of the mechanical construction is then to maintain the hydrophones at the wanted location with minimum movements around it. In addition, the array must be acoustically transparent in regards to the acoustic field it tries to describe. In practice underwater arrays that meet these requirements are obtained by using empty aluminum tubes in order to have both strength and acoustic transparency. From there the mechanical stability must be validated analytically and numerically to ensure precise positions for the hydrophones and therefore a good acoustic behavior of the array.

The contribution is organized as follow with Part II detailing the conception of the array. Part III shows the array mechanical validation from a theoretical point of view. Finally Parts IV and V describe the experimental setup and the results that validate the correct behavior of the array in real conditions, respectively.

II. Array Conception

A. Best hydrophones position definition

Acoustic array design relies on the possibility to compare the performances of different hydrophones configurations one against another. The performances typically used to make this comparison are the resolution defined by the array ability to separate two sources in space and the dynamic level which represents the array capacity to identify two sources that have different power levels. Consequently the array design methods try to combine these metrics to find the best configuration that yields a low resolution, ensuring a separation of two spatially close sources, along with a high dynamic, ensuring an identification of two sources with a large power level difference. However these two metrics do not evolve similarly, so a compromise must be reached in practice between resolution and dynamic to find out the best hydrophone positions. Among potential methods, the one chosen in this study takes into account the numerous constraints and it prevents a search in a large variety of cases. As a consequence the best configuration is searched hierarchically starting by complying only with industrial constraints and then scaling the shape chosen in this framework to find the final configuration within a set which corresponds to the research project scale.

The first industrial constraint is due to security reasons. Indeed a distance between the array deployment line and the working zone has to be respected. Besides the deployment means at disposal prevent the use of an array with a definite heading once set on the seafloor. It forces the use of an axisymmetric shape for the array in order to keep good performances for every heading obtained in practice. From a comparison of various axisymmetric geometries'resolution and dynamic, the conical tip down shape is selected for further optimization. This shape is composed of a hydrophone at the bottom of the array, a first circle of hydrophones at the middle height of the array and a wider second circle at the top height. The comparison is undertaken similarly than the one described for the next step, so only the second one is illustrated.

To respect the academic scale of the research project, the array must fit into a cube of 3 m side. The frequency band of the emitting source is scaled accordingly to [350 Hz; 7 kHz] to keep a similar resolution than in the industrial case in the resulting acoustic maps. The maximum number of hydrophone is fixed at 21. From there, among all the possible hydrophone configurations that can fit over a conical shape, 385 of them are selected corresponding to cases that are not too close one to another in order to sample as densely as possible the search space available while ensuring that they can be practically built. They are then compared by computing the resolution and dynamic for a simulated acoustic source located 50 m below and 75 m aside the array. These results are then averaged over the frequency band [800 Hz, 7 kHz]. It gives, for every tested configuration, a point in a plot average dynamic against average resolution allowing to visually compare their performances. This plot, displayed in Figure 1 with a reversed dynamic axis, allows to obtain the best arrays at the bottom left of the figure. Inverted grey triangles represent the 385 tested array while crosses represent small variations around the best one to check if better performances can be obtained.

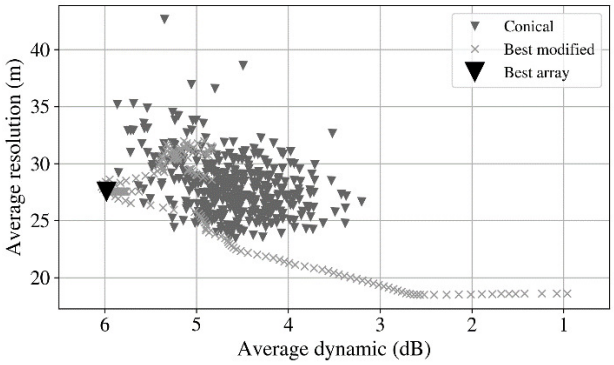

Figure 1: Scatter plot average resolution against average dynamic. Averages are computed over [800Hz; 7 kHz]. Grey triangles represent the 385 first tested configurations, the big black one is the best array in dynamic and crosses represent modifications around best array.

To choose the best array, a trade-off must be made between good resolution and good dynamic as they have contrary variations highlighted by the limit that appears at the bottom left of Figure 1. From an acoustic point of view, a dynamic of 8 dB is often a lower bound for an array to be considered as good, so regarding performances achievable with all the tested solution the one that yields the best average dynamic, of 6 dB here, is chosen.

B. Practical design

From given hydrophones position, a real array needs to be built. It means that a structure has to be designed to support the hydrophones, being rigid enough to ensure an accurate positioning while not interfering with the acoustic measurement.

1) Mechanical requirements

The respect of the geometry is required to ensure the wanted acoustic behavior. Nevertheless a perfect rigidity is not achievable in practice so an acoustic study is led in order to determine the needed accuracy in terms of hydrophone positioning. As presented in Figure 2, several errors are investigated: rotation of the circles compared to horizontal xy-plan (a), rotation around the vertical z-axis (b) and translation of the circles along vertical z-axis given by the margins in the sizes detailed in (a). The comparison of the performances of the array with or without errors suggests that:

- circles must stay horizontal with an error below 1°, ensuring to maintain dynamic at the same level than the case without error and bounding the localization errors below 1 m;
- rotation around the vertical must be limited to 1°, angle above which localization errors appear and dynamic is drastically degraded plummeting to 0 dB above 5 kHz;
- translation must be bounded below 30 mm to keep the localization errors below 1 m and the loss in dynamic below 1 dB.

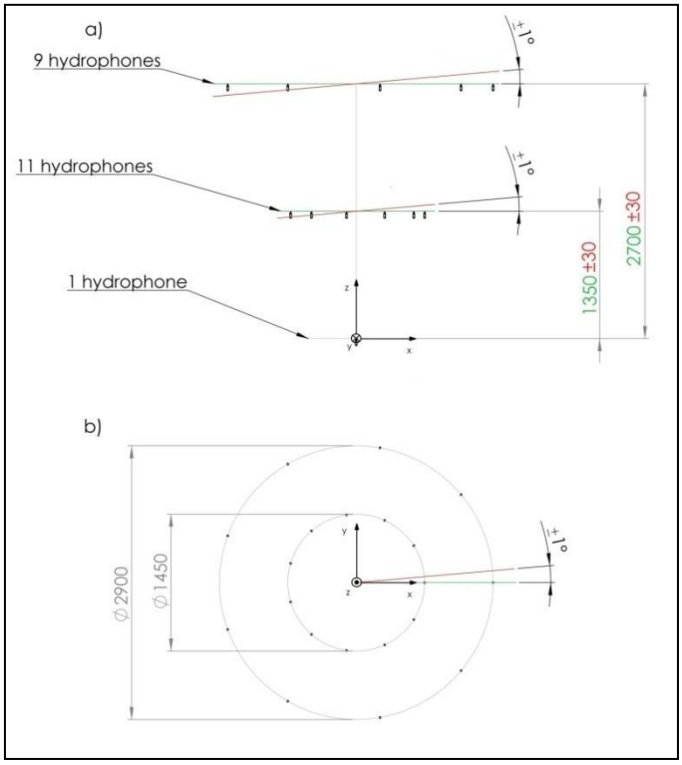

Figure 2 : Accuracy of hydrophone positioning. (a): side view of the array representing the allowable error around xy-plan to keep the hydrophones circles horizontal and allowable translation of the circles along vertical z-axis (b): top view of the array representing the allowable error around the vertical z-axis. Green represent the array as it should lie and red the array in the worst possible position.

2) Acoustic requirements

To respect mechanical requirements, a strong enough structure has to be designed. However, it generally goes hand in hand with a degradation of acoustic performances. It means that a compromise has to be found.

Plots displayed in Figure 3 allow to reach this compromise by representing the sound attenuation of various materials as a function of frequency [6]. Three different materials are studied, steel, aluminum and polyethylene, with for each of it, three different thickness 10 mm, 50 mm and 100 mm. The thicker the material the stiffer so for mechanical stability a thick material is searched. From there even if steel has very good mechanical performances, its acoustic behavior is very poor. Indeed, it attenuates drastically sound as its curves are decreasing very quickly when frequency increases. At the opposite, plastics such as polyethylene have good acoustic performances even with a high thickness, shown by flat curves, but in most applications mechanical properties are not strong enough. That is why aluminum with small thickness (10 mm) is the best compromise for this range of frequencies, achieving both stability and acoustic transparency goals.

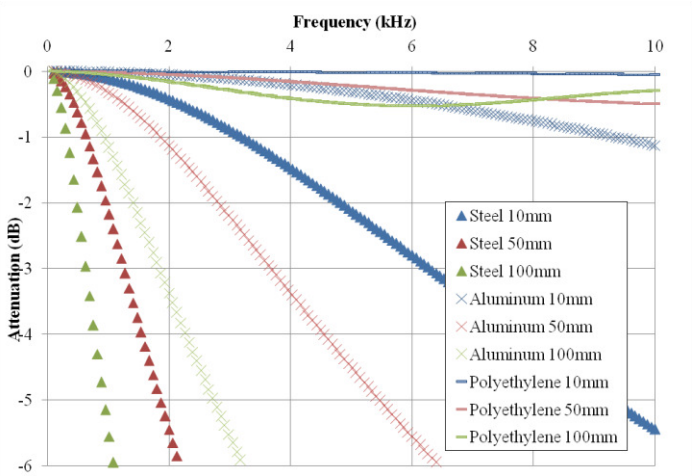

Figure 3: Acoustic attenuation of several materials as a function of frequency. The different curves are representing different materials (▲: steel, X: aluminum, ▬: polyethylene). For each marker the different colors represent different thickness (blue: 10 mm, red: 50 mm, green: 100 mm).

C. Applied stresses

1) Lift forces

During its mission, corresponding to the moment during which the array is measuring underwater sounds, the array is static somewhere between the surface and the sea ground. The only static forces that can act on the array are the weight in water of the ballast P_{Bw}, the weight in water of the ballast release system P_{Rw}, the thrust of the float $T$and the own weight in water of the array P_{Aw}.

The maximum force in mission F_M that the array has to stand is at the top of the array. According to Newton's laws of motion [7], it can be expressed as following:

$$F_M = -T. \quad (1)$$

But the harshest conditions are during deployment and recovery phases. When the array is at surface, it spends some time hanged at the stern of the boat. In this configuration, the array has to stand the weight in water of the ballast P_{Bw}, the

weight in water of the ballast release system P_{Rw} and its own weight in air P_A. However, with bad weather conditions, the boat can move which induces an additional force due to acceleration a.

According to Newton's laws of motion, the resulting force at surface F_S that the array has to stand can be expressed as following:

$$F_S = k.(P_A + P_{Bw} + P_{Rw}). \quad (2)$$

Where:

$$k = \frac{a+g}{g}. \quad (3)$$

With g the gravity of earth (m/s^2). k can be considered as a safety factor.

2) Drag forces

During deployment and recovery phases, the array can suffer of drag forces from the surface to the sea ground. These drag forces have to be known and controlled to avoid over constraints on the array which could change hydrophones position or damage the structure.

In fluid dynamics [8], drag can be evaluated with the following drag equation:

$$F_D = \frac{1}{2}\,\rho\, C_D\, A\ v^2. \quad (4)$$

$F_D$represents the drag force (N), ρ the fluid density (kg/m^3), v the speed of the object (m/s), A the cross sectional area (m^2) and C_D the drag coefficient.

Drag coefficient depends on the shape of the object and on the Reynolds number:

$$R_e = \frac{v\,D}{\nu}. \quad (5)$$

R_e is the Reynolds number, D the characteristic dimension of the object (m) and ν the kinematic viscosity (m^2/s). For our range of speed, C_D can be considered as a constant.

In our case, sea water density ρ and array speed v are the same for the whole array; however, cross sectional area A and drag coefficient C_D change for each part of it because of shapes and dimensions. Therefore, drag calculation can be decomposed in several sub-forces F_{Di} with their own C_{Di} and A_i associated.

By corollary, equation (4) gives:

$$F_D = \sum(F_{Di}) = \frac{1}{2}\,\rho \sum(C_{Di}A_i)\ v^2. \quad (6)$$

3) Pressure forces

In deep sea water, one of the major problem is the pressure. As much as possible, materials and devices must be pressure resistant and waterproof. When it is not possible, devices that cannot stand the pressure or have to remain in air must be integrated in a watertight and pressure-resistant enclosure.

D. Mechanical realization

From the simulated design and given the applied stresses, the mechanical structure presented in Figure 4 has been conceived. All the structure is built on two central aluminum beams. For each hydrophone circle, aluminum machined plates have been fitted and adjusted in the beams. Each ring of hydrophone is linked to the machine plate using U profile spokes. Finally, shapes to receive the hydrophones are directly made into aluminum sheet metal ring to control their position at best. This mechanical design coupled with controlled industrial processes, ensure to respect required tolerances and a good reliability about the hydrophone positions given.

In order to avoid any influence of lift forces on hydrophones position, hanging rings (c) for ballast and float or fixing points for other accessories have been done on the central beam. All efforts pass only through the central beam. Therefore, its size has been largely overestimated to deal with all the unexpected. In regards of formula (4), the only way to reduce drag forces is to act on cross sectional area A of each parts. For this reason, every parts, and especially rings, has been perforated, to let the water go through the array. Furthermore, this action reduces the amount of aluminum, limiting weight and acoustic disturbances.

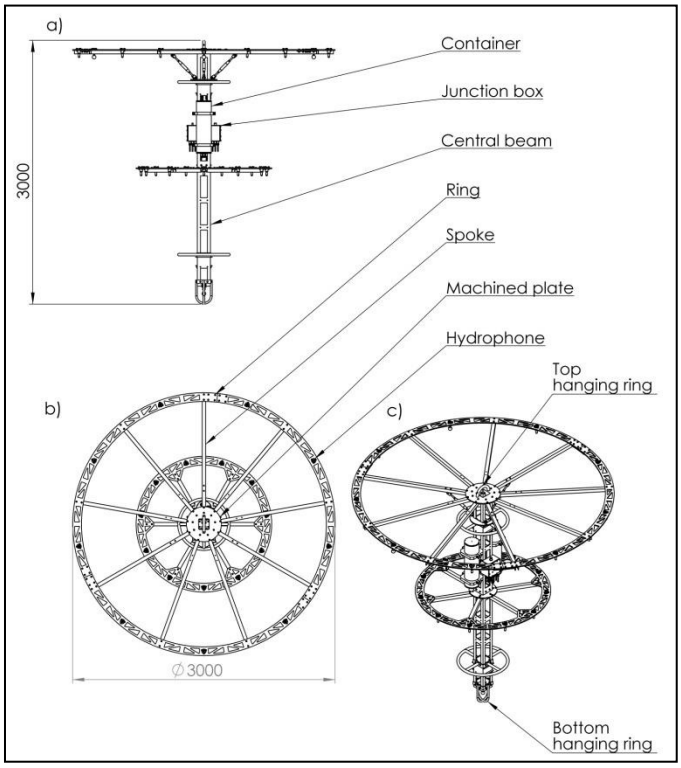

Figure 4 : Acoustic array diagram. Arrows identify designations of each part and values are overall dimensions in mm. (a) Side view of the array (b) Top view (c) Isometric view.

Most of parts are pressure resistant and waterproof. Aluminum structure has no captive air, hydrophones and cables are overmoulded and a lot of connections have been done in two equipressure junction boxes filled with oil, visible on Figure 4 (a). For the rest of devices that cannot be in contact with water or withstand the pressure, two watertight pressure

resistant containers have been manufactured (a). One has been filled with batteries, the other with all electronic equipment. Containers diameter and thickness have been defined by calculation in function of pressure and material properties.

III. Array validation

Before building physically the array, structure must be validated against the expected stresses applied during its use.

A. Preamble

In order to check if the structure can withstand the constraints, the forces acting on the system have to be known. To reach this aim, weights and thrust have to be estimated along with array speed v during deployment and recovery phases.

1) Weights and thrust

The weight in air P_A and in water P_{Aw} of the array are respectively estimated at 1450 N and 700 N. The weight in air P_R and in water P_{Rw} of the ballast release system are estimated at 300 N and 200 N.
To bring back the array to the surface, a sufficient remaining thrust T_S have to be chosen, with:

$$T_S = P_{Aw} + P_{Rw} + T. \quad (7)$$

The aim is to have a remaining thrust about -600 N, so the thrust T must be about -1500 N.

To make the array able to sink and to have a good anchorage to the sea ground, a sufficient remaining weight P_S have to be choosen, with:

$$P_S = P_{Aw} + P_{Rw} + P_{Bw} + T. \quad (8)$$

The aim is to have a remaining weight about 600 N, so the weight in water of the ballast P_{Bw} must be about 1200 N.

2) Array speed

During deployment, after an accelerated phase, the array reaches a limit speed v_{ld}, so the sum of forces on the array are equilibrated with the drag forces F_{Dd}.

According to Newton's laws of motion, the sum of forces in deployment is:

$$P_{Aw} + P_{Rw} + P_{Bw} + T - F_{Dd} = 0. \quad (9)$$

Moreover with (8):

$$P_S - F_{Dd} = 0. \quad (10)$$

With equation (6) on F_{Dd}, the limit speed in deployment v_{ld} can be expressed as following:

$$v_{ld} = \sqrt{\frac{P_S}{\frac{1}{2}\,\rho \sum(C_{Di}A_i)}}. \quad (11)$$

During recovery, after an accelerated phase, the array reaches a limit speed v_{lr}, so the sum of forces on the array are equilibrated with the drag forces F_{Dr}.

According to Newton's laws of motion, the sum of forces in recovery is:

$$P_{Aw} + P_{Rw} + T + F_{Dr} = 0. \quad (12)$$

Moreover with (7):

$$T_S + F_{Dr} = 0. \quad (13)$$

With equation (6) on F_{Dr}, the limit speed in recovery v_{lr} can be expressed as following:

$$v_{lr} = \sqrt{\frac{-T_S}{\frac{1}{2}\,\rho \sum(C_{Di}A_i)}}. \quad (14)$$

In our case, sea water density ρ is 1026 kg/m^3 and $\sum(C_{Di}A_i)$ is estimated in function of shapes and dimensions of each parts on the array. In regards to section III.A.1), both P_S et $-T_S$ have been chosen equal to 600 N.

So, limit speed in both cases can be estimated at 0.75 m/s.

B. Mechanical simulations

Mechanical simulations have been carried out with finite element analysis [9].

Aluminum yield strength is estimated at 160 MPa. To keep the array out of any damage, the maximum constraint must stay under this value.

1) Lift forces validation

To represent the array hanged by its top hanging ring and with a load at the bottom hanging ring, a simulation has been done and is represented in Figure 5. A static upper point is represented by green arrows and a force at the lowest point is represented by purple arrows.

The aim is to find the maximum force the array can withstand, with constraints in array staying below aluminum yield strength of 160 MPa. On simulation Figure 5, yield strength is reached for a maximum load of $10458\,N$. As a comparison, with the values estimated in section III.A.1), lift forces can be calculated. The maximum force in mission F_M is about 1500 N, according to equation (1), and the resulting force at surface $F_S = k.2850\,N$, according to equation (2). These results means, the maximum load found by simulation is seven times higher than the maximum force in mission F_M, and corresponds to a safety factor $k = 3.7$ with the resulting force at surface F_S.

The colors represent the constraint in MPa, going from blue (0 MPa) to red, the maximum constraint (156.8 MPa). At maximum load, most of the array stays blue (a). This reveals that central beam and, above all, strokes and rings do not fill any significant constraints. Only top and bottom hanging rings suffer of constraints. The maximum is reached at the bottom hanging ring (b) allowing it to act like a fuse and drop the ballast in case of over constraints to save the array.

To conclude, All these safety margins allow a comfortable use of the array in real conditions.

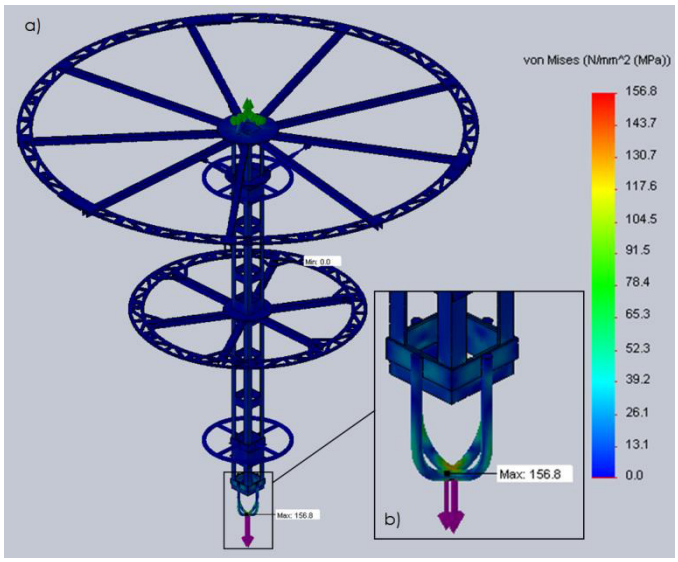

Figure 5: Maximum constraints of array subjected to lift forces. Color gradient represents constraints in MPa, from blue to red. Green arrows are the static point localization and purple arrows represent the lift forces applied onto the array. This simulation has as input data, a force of 10458 N. (a): whole array (b): zoom on bottom hanging ring with the maximum constraint.

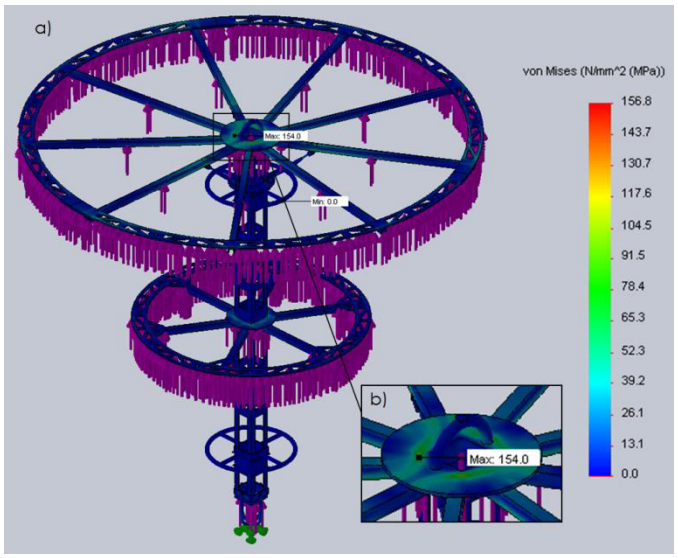

Figure 6 : Maximum constraints of array subjected to drag forces. Green arrows are the static point localization. Purple arrows represent drag forces distributed according to parts shapes. Drag forces depends on the speed chosen. This simulation has as input data, a speed of 1.8 m/s. Color gradient represents constraints in MPa, from blue to red. (a): whole array. (b): zoom on top machine plate of largest ring where the maximum is reached.

2) Drag forces validation

On simulation displayed in Figure 6, the bottom hanging ring has been fixed, represented by green arrows. Drag forces F_{Di}, represented by purple arrows, have been applied at each part in function of theirs drag coefficient C_{Di} and cross sectional area A_i. It allows to simulate the array going down to the sea ground.

The aim is to find the maximum speed the array can reach, with constraints staying below yield strength. To simulate action of speed on the array, F_{Di} are applied on each part. On simulation Figure 6, yield strength is reached for a maximum speed of 1.8 m/s, corresponding to a cumulative drag force F_D of 3070 N. According to part III.A.2), the limit speed v_l of our system is about 0.75 m/s, which means that the speed found by simulation is 2.4 times higher than the limit speed v_l estimated. Moreover, drag force F_D evolves like the square of the speed, so at 0.75 m/s F_D is 5.8 times lower than the simulation. So the array can again be used in secured conditions.

As on Figure 5, the colors on Figure 6 represent the constraint in MPa. At this maximum speed, most of the array stays blue (a). Most of constraints are located at junctions of machined plates and spokes and maximum is reached at the largest ring (b). Indeed, most of drag forces are located on the rings and they all act on the center through the spokes.

IV. Experimental Configuration

An experiment is conducted to study the behavior of the built array in real conditions. It has been made in the Mediterranean Sea in April 2018 in a shallow water zone of 104 m depth. The configuration is represented in Figure 7 with the array immersed at 51 m and the acoustic source placed at a distance x = 8 m and y = 59 m of it and immersed at 80 m depth.

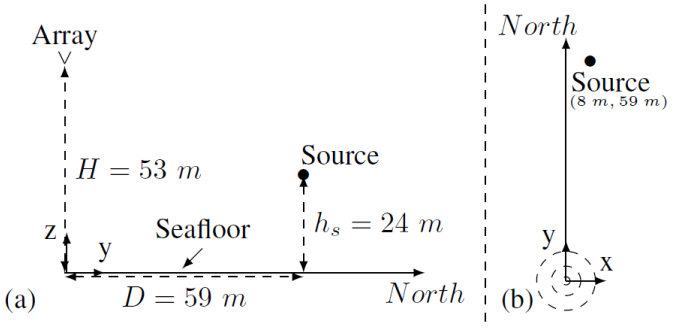

Figure 7: Experimental configuration.(a): side view the array is located at (0 m, 0 m, 53m), the source at (8 m, 59 m, 24 m).(b): top view with the array represented by dashed circles at (0 m, 0 m) and the source by a bullet point at (8 m, 59 m).

The acoustic source sequence is composed of 5 sinus of 10 s between 3 and 7 kHz with a step of 1 kHz. Every signal is followed by a silence of 1 s and sequence is repeated over time.

From there the goal of the acoustic localization is to find the source in a plan parallel to the seafloor and at the source height (24 m). To do so this plan, chosen of size 200 m x 200 m centered on the array, is discretized by step of 0.5 m and the acoustic imagery methods computed for every node of the obtained grid. Consequently the shown acoustic results must be understood as a top view of the configuration for a plan at 24 m height from the seafloor.

V. Experimental results

A. Mechanical behavior

1) Hydrophones position

To validate that hydrophones position do not change along time, position controls have been done between each manipulations of the array. These measurements have been realized with Leica Disto S910. This devise is a laser distance meter which can give 3D positioning data of several points, and then create a 3D file. The compilation of these data makes possible to compare hydrophones position between each measurement.

Along manipulations for the first mission, measurements have been done at three instants. After mounting of the array (T_1), three measurements ($T_{1.1}$,$T_{1.2}$,$T_{1.3}$) have been conducted. After test deployment in pool (T_2), two measurements ($T_{2.1}$,$T_{2.2}$) have been made. Finally, after deployment in sea (T_3), two measurements ($T_{3.1}$,$T_{3.2}$) have been done.

Figure 8 presents average and standard deviation for each measurement, of three dimensional error between measured positions and reference positions of hydrophones.

The average on error of hydrophone positions is 2.2 mm, the standard deviation is 1.2 mm and the maximum error is 6.3 mm. In regards to mechanical requirements, these results are in the tolerance, which means that there is no significant displacement. Therefore, the reliability of the given positions is ensured.

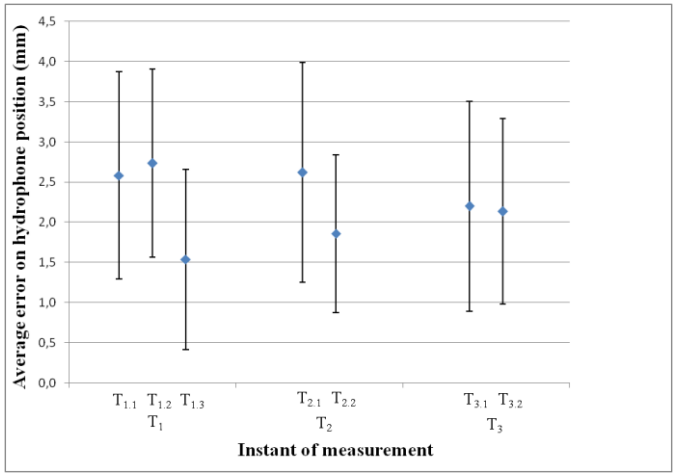

Figure 8: Average with standard deviation bars of three dimensional error between measured positions and reference positions of hydrophones, at different time of measurements. (T_1): three measurements after array mounting. (T_2): two measurements after test deployment in pool. (T_3): two measurements after mission deployment in sea.

2) Lift forces

Before the mission, real weights and thrusts have been measured in air and in sea water. Table 1 gathers these data.

Table 1: Measured weights and thrusts before the deployment both in air and in sea water

Weights and thrusts	In air (N)		In sea water (N)	
	Theory	Measure	Theory	Measure
Array weight P_A	1450	1398	700	672
Ballast release system weight P_R	300	265	200	167
Ballast weight P_B	-	1403	1200	1222
Float thrust T	-	-	-1500	-1432
Remaining thrust T_S	-	-	-600	-594
Remaining weight P_S	-	-	600	629

Weights and thrusts measured are very close to theory. With these data, maximum force in mission F_M is 1432 N and resulting force at surface $F_S = k.2061\,N$. So the array behaves as expected and can be used safely for its mission.

3) Drag forces

During the first mission, deployment and recovery speed which have been measured was 0.28 m/s and no damages or change in hydrophones position appeared.

However the speed that the array should have reached should be around 0.75 m/s. Indeed, the array has not been thrown from the boat to the sea ground with its own speed but it has been dropped with a mooring line, which means that the array went down at the boat winch speed.

During the following mission, the array will be thrown from the boat. With the measured data gathered in Table 1, the limit speed in deployment v_{ld} should be about 0.77 m/s and the limit speed in recovery v_{lr} should be about 0.74 m/s.

B. Acoustic behavior

Once the mechanical behavior is validated, the acoustic one can be studied to check if the array answers correctly to the goal it has be built for: localizing acoustic sources. The Conventional Beam Forming (CBF) [10] method is used to perform localization and is given in Eq. 1:

$$CBF_g = 20\log\left(\frac{\boldsymbol{g}^*\boldsymbol{\Gamma}\,\boldsymbol{g}}{Tr(\boldsymbol{\Gamma})\|\boldsymbol{g}\|^2}/P_{ref}^2\right). \quad (15)$$

With $\boldsymbol{\Gamma}$ corresponding to the cross spectral matrix computed from the data, $\boldsymbol{g}$ a steering vector corresponding to a specific grid point, $Tr(.)$ the trace of a matrix, $.^*$ the Hermitian transposition and $P_{ref} = 10^{-6}$ Pa, the underwater reference pressure.

This version of CBF gives a normalized value for the maximum of the map at 120 dB which gives the estimation of the source localization on the computation grid.

The CBF result for the experimental setup is given in Figure 9 with a source emitting at 7 kHz.

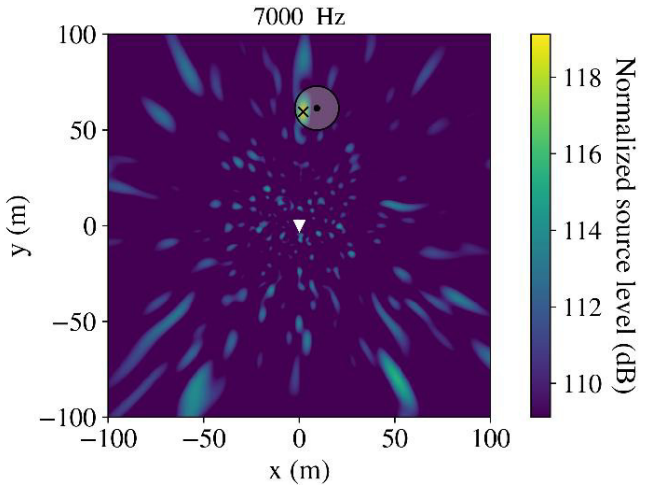

Figure 9: CBF map computed from the experimental data at 7 kHz. ▼: array position at (0 m, 0 m, 53 m). ●: GPS boat position at (9 m, 61 m, 104m) (104m is the water depth). ×: estimated source position at (2 m, 60 m, 24 m). The uncertainty zone is represented by the whitened circle and has an 11.5 m radius.

The source is found at the position (x = 2 m, y = 60 m) which relies in the uncertainty zone represented by the whitened area in the map. This uncertainty is due to the GPS accuracy of the boat combined with relative positioning of the source in comparison with the boat like verticality of the source below it or depth precision. This result validates the acoustic array behavior in real conditions.

As a comparison, a result of simulation map at 7 kHz is given in Figure 10.

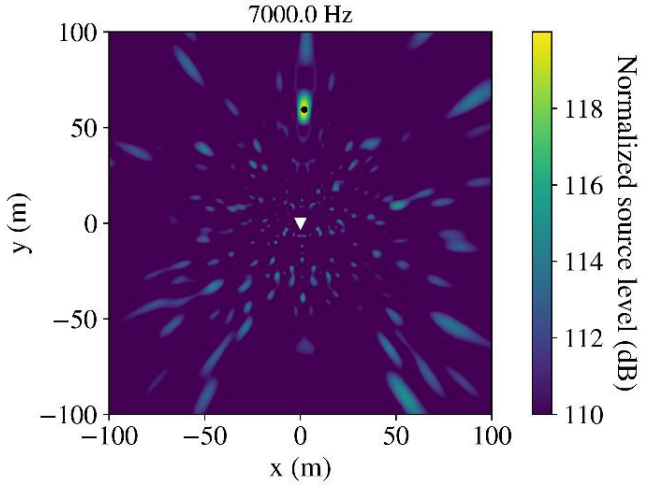

Figure 10: CBF map computed from simulated data at 7 kHz and a source at x = 2 m, y = 59.5 m. ▼: array position at (0 m, 0 m, 53 m). ●: source position at (2m, 60 m, 24 m).

Both maps are really similar which confirms the respect of the design during the construction step. Indeed the similarity between simulated and real maps show that hydrophones are really located where they thought to be and moreover the array structure does not disturb the surrounding acoustic field.

VI. Conclusion

As deep sea mining starts to be carried out by companies, the need for controlling the noise emitted by this kind of industry occurs. The research project Abysound answers this issue by proposing, at laboratory scale, a monitoring system that is able to localize and quantify deep sea underwater acoustic sources representing the excavation machines used in mining sites. From there impact maps can be generated to show stresses applied on the marine life.

Specifically in this contribution, the design of the acoustic array used for localization is detailed. At first the hydrophones position are determined using a hierarchical optimization that allows to take into account the numerous constraints the array must respect. This design step ends up with a conical shape with the tip down and the 21 available hydrophones disposed over two hydrophone circles at respectively 1.35 m and 2.7 m height with 1.45 m and 2.9 m diameter. Then this array is built in agreement with all the mechanical and acoustical requirements such an array has to deal with. Consequently, it is manufactured around a central beam that absorb all the static constraints and the hydrophones rings are connected to it using spokes on which very few constraints are applied. This structure is then validated by finite elements computations with safety margins in order to be sure to use the array without any risk in real conditions.

An experimental validation is led thanks to a shallow water deployment in Mediterranean Sea in April 2018. Results show agreement between estimated constraints and measured ones as well as a robust positioning of the hydrophones with a three dimensional error bounded below 6.3 mm at maximum.

Finally acoustic imagery results show an acoustic source found where it should lie with an experimental map really close to a corresponding simulated one. It allows to conclude on the good behavior of the array and to trust the accurate construction of it at each step.

Acknowledgment

This work is supported by BPI and TPM for Abysound project fundings. The authors would like to thank all the partners of Abysound project: Naval Group, MicrodB, Osean, Semantic TS, IFREMER, Gipsa-Lab, LMA and UTLN.

This work was supported by the LABEX CeLyA (ANR-10-LABX-0060) of Université de Lyon, within the program "Investissements d'Avenir" (ANR-16-IDEX-0005) operated by the French National Research Agency (ANR).

References

[1] G. Spanoli, S. Miedema, C. Herrmann et al., "Preliminary design of a trench cutter system for deep-sea mining applications under hyperbaric conditions", in IEEE Journal of Oceanic Engineering, vol 41(4), pp. 930-943, 2016.

[2] S. Gollner, S. Kaiser, L. Menzel et al., "Resilience of benthic deep-sea fauna to mining activities", in Marine Environmental Research, vol 129, pp. 76-101, 2017.

[3] R.L. Haupt, “Thinned arrays using genetic algorithms”, in IEEE Transactions on Antennas and Propagation, vol 42(7), pp. 993-999, 1994.

[4] M.R. Bai, J.H. Lin and K.L. Liu, “Optimized microphone deployment for near-field acoustic holography: to be, or not to be random, that is the question”, Journal of Sound and Vibration, vol. 329(14), pp. 2809-2824,2010.

[5] E. Sarradj, “A generic approach to synthesize optimal array microphone arrangements”, in Berlin Beamforming Conference 2016, p. 1-12, 2016.

[6] L.M. Brekhovskikh, "Waves in layered media", in Academic Press, 1980.

[7] J.B. Marion and S. Thornton, "Classical Dynamics of Particles and Systems", in Academic Press, 1995.

[8] G. Batchelor, "An introduction to fluid dynamics", in Cambridge Mathematical Library, 2000.

[9] G. Allaire and A. Craig, "Numerical Analysis and Optimization: An Introduction to Mathematical Modelling and Numerical Simulation", in oxford science publications, 2005.

[10] G. Elias, “Experimental techniques for source location”, Von Karman Institute, Lecture Series, 1997.